Acta Crystallographica Section D
Biological Crystallography
ISSN 0907-4449

Use of an in-house approach to study the three-dimensional structures of various outer membrane proteins: structure of the alcaligin outer membrane transporter FauA from *Bordetella pertussis*

Karl Brillet,[a] Ahmed Meksem,[a,b] Emmanuelle Lauber,[c] Cornelia Reimmann[d] and David Cobessi[a,b]*

[a]Institut Gilbert-Laustriat, UMR7175 CNRS/Université Louis Pasteur, Strasbourg I, Département Récepteurs et Protéines Membranaires, Ecole Supérieure de Biotechnologie de Strasbourg, BP 10413, F-67412 Illkirch, France, [b]Institut de Biologie Structurale Jean-Pierre Ebel, CEA–CNRS–Université Joseph Fourier, 38027 Grenoble, France, [c]Laboratoire des Interactions Plantes Micro-organismes (LIPM), UMR CNRS–INRA 2594/441, F-31320 Castanet-Tolosan, France, and [d]Département de Microbiologie Fondamentale, Université de Lausanne, Bâtiment Biophore, Quartier UNIL-Sorge, CH-1015 Lausanne, Switzerland

Correspondence e-mail: david.cobessi@ibs.fr

Received 14 October 2008
Accepted 16 January 2009

PDB Reference: FauA, 3efm, r3efmsf.

Bordetella pertussis is the bacterial agent of whooping cough in humans. Under iron-limiting conditions, it produces the siderophore alcaligin. Released to the extracellular environment, alcaligin chelates iron, which is then taken up as a ferric alcaligin complex *via* the FauA outer membrane transporter. FauA belongs to a family of TonB-dependent outer membrane transporters that function using energy derived from the proton motive force. Using an in-house protocol for membrane-protein expression, purification and crystallization, FauA was crystallized in its apo form together with three other TonB-dependent transporters from different organisms. Here, the protocol used to study FauA is described and its three-dimensional structure determined at 2.3 Å resolution is discussed.

1. Introduction

The first crystal structure of a membrane protein, the photosynthetic reaction centre of *Rhodopseudomonas viridis*, was solved at 3 Å resolution more than 20 years ago (Deisenhofer *et al.*, 1985). Since then, no more than 400 crystal structures of membrane proteins have been determined (see http://blanco.biomol.uci.edu/Membrane_Proteins_xtal.html), while the Protein Data Bank contains more than 50 000 structures of macromolecules (soluble proteins, DNA, RNA, large macromolecular complexes *etc.*). This large difference mainly results from difficulties in obtaining large quantities of pure membrane proteins suitable for crystallization (Loll, 2003). Moreover, crystals of membrane proteins often diffract X-rays poorly.

Gram-negative bacteria are surrounded by two lipid bilayers that reinforce cell impermeability. While small molecules such as ions or sucrose can cross the outer membrane (OM) by passive diffusion through porins, the transport of molecules larger than 600 Da or molecules that are present at low concentrations such as iron, haem, maltose, sucrose, vitamin B_{12} or nickel (Schauer *et al.*, 2008) takes place *via* TonB-dependent transporters (TBDTs) using energy derived from the proton motive force of the inner membrane. This is achieved through an interaction between the TonB periplasmic part of the inner membrane energy-transducing complex TonB–ExbB–ExbD and the so-called TonB box of the TBDT, a conserved sequence located at its N-terminus (Wiener, 2005). The molecular mechanisms of transport and the signal transduction necessary for energy transfer are still unknown. A genome survey revealed that more than 70% of all Gram-negative bacteria have genes for TBDTs (Blanvillain *et al.*, 2007) and many species can express several TBDTs (Blanvillain *et al.*, 2007). In order to better understand the molecular mechanisms of these transporters, we undertook

crystallographic studies of FpvA and FptA, which are required for siderophore-mediated iron uptake in *Pseudomonas aeruginosa* (Cobessi, Celia, Folschweiller *et al.*, 2004, 2005; Cobessi, Celia & Pattus, 2004, 2005). Their structure consists of a C-terminal domain that folds into a 22-stranded transmembrane β-barrel which is filled by a so-called plug domain. The structures of the *P. aeruginosa* TBDTs thus resemble those of all other crystallized TBDTs involved in siderophore uptake (Ferguson, Hofmann *et al.*, 1998; Ferguson *et al.*, 2002; Locher *et al.*, 1998; Buchanan *et al.*, 1999, 2007) and vitamin B_{12} uptake (Chimento *et al.*, 2003).

As part of our efforts towards understanding the crystallization of membrane proteins and membrane transport across the outer membrane of Gram-negative bacteria, we developed a strategy from cloning to crystallization in order to facilitate the production, purification and crystallization of TBDTs. This easy handling protocol developed for TBDTs could probably be applied to other membrane proteins from Gram-negative and Gram-positive bacteria. Our strategy overcomes the bottlenecks of structural studies on membrane proteins, allowing us to collect X-ray data for all the selected targets: the alcaligin TBDT from *Bordetella pertussis*, the sucrose TBDT from *Xanthomonas campestris* pv. *campestris*, the enantio-pyochelin TBDT from *P. fluorescens* and the haem TBDT from *Shigella dysenteriae*. These four TBDTs share between 14.4% (SuxA/ShuA) and 24.9% (FauA/FetA) sequence identity. Here, we mainly detail the protocol used to study the alcaligin outer membrane transporter FauA from *B. pertussis*, for which we solved the three-dimensional structure at 2.3 Å resolution. *B. pertussis* is a Gram-negative human pathogen that inhabits the respiratory mucosa and produces the macrocyclic dihydroxamate siderophore alcaligin to acquire iron (Brickman & Armstrong, 1999). After binding to iron(III), the ferric alcaligin is translocated across the outer membrane by FauA.

2. Materials and methods

2.1. Bacterial strains

DNA manipulations were carried out in *Escherichia coli* Top10 [*F*$^-$ *mcrA* Δ*(mrr-hsdRMS-mcrBC)* φ*80lacZ*Δ*M15* Δ*lacX74 recA1 araD139* Δ*(ara-leu)7697 galU galK rpsL (StrR) endA1 nupG*] and FauA was overexpressed in *E. coli* BL21 (DE3) [*F*$^-$ *ompT hsdS*$_B$*(r*$_B^-$*m*$_B^-$*) gal dcm (DE3)*].

2.2. Expression vector

The DNA encoding FauA from *B. pertussis* (without the 35-residue signal sequence) was amplified by PCR. The forward primer of the first fragment F1 (5′-GTCAGATATC**CAGGAAGCGCGAACG**-3′) contained the complementary part for an *Eco*RV site (underlined) and codons for residues 36–40 of the mature FauA protein (bold). The reverse primer (5′-GCTAGGATCC**GGCGCGGCGCCAGTC**-3′) for F1 contained a *Bam*HI site (underlined) and anticodons for residues 423–427 of mature FauA (bold). The forward primer of the second fragment F2 (5′-GATCGGATCC*CATCACCATCATCACC-AT***CACATCCAAGAGCCCAGC**-3′) contained a *Bam*HI site (underlined) that introduces two residues GS, a DNA sequence encoding a His_6 tag (italicized) and codons for residues 428–433 of the mature FauA protein. The reverse primer F2 (5′-GTCAAAGCTT*TCA***ATACTGCGCCCGCAA**-3′) contained a *Hin*dIII site (underlined), a stop anticodon (italicized) and anticodons for residues 730–734 of the mature FauA. The PCR products were cloned in pET20b (Novagen). *E. coli* Top10 cells were transformed with the resulting expression plasmids pET20b-FauAF1 and pET20b-FauAF2. All cloning steps were verified by DNA sequencing at the IGBMC facility, Illkirch, France.

The FauAF2 fragment was removed from plasmid pET20b-FauAF2 and introduced into pET20b-FauAF1 using *Bam*HI and *Hin*dIII restriction sites. *E. coli* BL21 (DE3) cells were transformed with the resulting construct. Thus, this construct encodes a protein in which the native *B. pertussis* signal peptide is replaced by the native N-terminal *pelB* signal sequence of *E. coli* to target FauA into the outer membrane. The His_6 tag in loop L5 allowed rapid purification of the FauAH6L5 protein.

2.3. Expression and purification

E. coli BL21 (DE3) expressing FauAH6L5 was isolated on Luria Bertani–ampicillin (LB–ampicillin; 100 µg ml^{-1} ampicillin) plates and a 35 ml LB–ampicillin preculture was grown overnight at 310 K and 220 rev min^{-1}. The subculture was then used to inoculate a 1 l LB–ampicillin culture, which was incubated for another 2 h until the optical density (OD_{600}) reached 0.6. Expression of the recombinant protein was induced by adding 1 m*M* isopropyl β-D-1-thiogalactopyranoside (IPTG) at 310 K. After 3 h, the cells were harvested by centrifugation for 20 min at 10 000*g*.

The bacterial pellets were resuspended in 50 m*M* Tris–HCl pH 8.0 and disrupted by two sonication steps. The membrane pellet was deposited on a four-step sucrose gradient and centrifuged overnight at 188 000*g* (Beckman SW41 rotor) to observe the location of the TBDTs in the membranes. The different parts of the gradient were deposited on an SDS gel to separate the proteins before Western blotting. FauAH6L5 was purified after incubation of the membranes with 1%(*w*/*v*) sodium *N*-lauroylsarcosine, which led to solubilization of the cytoplasmic membranes. Intact outer membranes containing FauAH6L5 were pelleted by centrifugation at 125 000*g* for 40 min in a Beckman Ti45 rotor. To extract FauAH6L5, the pellet of outer membranes was solubilized at room temperature with 50 m*M* Tris–HCl pH 8.0, 500 m*M* NaCl and 7%(*v*/*v*) octylpolyoxyethylene (octyl-POE; Bachem) and subsequently centrifuged at 117 000*g* for 20 min in a Beckman Ti70 rotor. The supernatant was applied onto a HisTrap column (Amersham) equilibrated in 50 m*M* Tris–HCl pH 8.0, 500 m*M* NaCl, 20 m*M* imidazole and 1% octyl-POE. The protein was eluted with a linear gradient of 20–500 m*M* imidazole in 50 m*M* Tris–HCl pH 8.0, 500 m*M* NaCl and 1% octyl-POE. The fractions containing FauAH6L5, as determined by SDS–PAGE, were pooled, concentrated and dialyzed against 50 m*M* Tris–HCl

pH 8.0 and 1% octyl-POE by ultrafiltration and loaded onto a HiTrapQ column (Amersham) equilibrated in 50 m*M* Tris–HCl pH 8.0 and 1% octyl-POE. FauAH6L5 was eluted with a linear gradient of 0–1 *M* NaCl in 50 m*M* Tris–HCl pH 8.0 and 1% octyl-POE.

2.4. Crystallization experiments

The pure fractions containing FauAH6L5 were pooled and dialyzed against 10 m*M* Tris–HCl pH 8.0 and either 0.75% C_8E_4, 0.75% C_8E_5 (Bachem) or 1.4% β-octylglucoside (Anatrace). The initial crystallization experiments were performed using a Cartesian Honeybee system at SBGP (Illkirch, France) by mixing 100 nl protein solution at a protein concentration of 10 mg ml^{-1} with 100 nl crystallization solution. The MbClass Suite, MbClass II Suite, Classics Suite and Classics Lite Suite from Qiagen were tested with the three detergents. Optimizations of the crystallization conditions were performed in Linbro plates using the sitting-drop vapour-diffusion method at 293 K.

2.5. Data collection

Diffraction data were initially collected using synchrotron radiation on BM30A at the ESRF (Roth *et al.*, 2002) at 3 Å resolution using an ADSC Q315r CCD detector ($\lambda = 0.9797$ Å). The resolution was extended to 2.3 Å on PROXIMA-1 at SOLEIL using a MAR flat panel ($\lambda = 0.9789$ Å). In both cases the data were collected using one crystal at 100 K and were integrated and scaled using *XDS* (Kabsch, 1993).

2.6. Structure resolution

The phase problem was solved by molecular replacement using *MOLREP* (Vagin & Teplyakov, 1997) from the *CCP*4 suite (Collaborative Computational Project, Number 4, 1994) with FpvA (Brillet *et al.*, 2007) as a molecular model after replacing the nonconserved residues by alanine residues and after removing non-aligned parts of the sequences. The first model was refined using the data collected on BM30A at 3 Å resolution and the model was then rebuilt at 2.3 Å resolution using *Coot* (Emsley & Cowtan, 2004) and refined by energy minimization and molecular dynamics using *CNS_SOLVE* 1.2 (Brünger *et al.*, 1998) and by restrained maximum-likelihood least-squares techniques in *REFMAC* 5.2 (Murshudov *et al.*, 1997) from the *CCP*4 suite (Collaborative Computational Project, Number 4, 1994). At the end of the refinement, water molecules and sulfate ions were added and a simulated-annealed composite $3F_o - 2F_c$ electron-density map was calculated using *CNS_SOLVE* to check the model. The model was also checked using *PROCHECK* and *WHATCHECK* (Laskowski *et al.*, 1993; Hooft *et al.*, 1996).

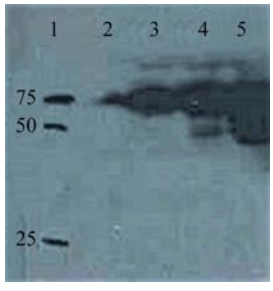

Figure 1
Induced expression of one selected TBDT in *E. coli*. Membrane fractions from induced cells were prepared as described in §2 and identified by Western blot analysis using a monoclonal antipolyhistidine antibody (Sigma): lane 1, ladder (kDa); lane 2, supernatant; lane 3, inner membrane; lane 4, intermediate fraction; lane 5, outer membrane.

3. Results and discussion

3.1. Construction and analysis of the expression plasmid

To overexpress FauA in *E. coli*, we used pET20b, which codes for the *E. coli* signal peptide PelB required for targeting heterologous proteins to the outer membrane. As we were working on several TBDTs, we first inserted the His_6 tag into the N-terminal part of one particular TBDT. However, Western blot analysis of inner and outer membrane fractions obtained by ultracentrifugation on a sucrose gradient revealed that the overexpressed TBDT had accumulated in the inner membrane (data not shown). This accumulation probably resulted from nonrecognition of the signal peptide by the inner membrane secretion system owing to the presence of the His_6 tag inserted immediately downstream. We thus decided to insert the His_6 tag into one of the extracellular loops, *i.e.* loop L5, following the cloning protocol described for the FauA receptor in §2. FhuA was also cloned with a His tag inserted in an extracellular loop (Ferguson, Breed *et al.*, 1998). After 3 h of overexpression at 310 K, most of the protein was found in the *E. coli* outer membrane (Fig. 1). The other TBDT expression plasmids, which will be described elsewhere, were therefore constructed in a similar way, *e.g.* by inserting the His_6 tag into one of the extracellular loops.

3.2. Obtaining large quantities of membrane proteins

In order to limit the number of purification steps, we purified the TBDTs by a two-step procedure only, *i.e.* affinity and anion-exchange chromatography; an additional gel-filtration step did not improve the crystallization conditions. Using this two-step approach, we obtained pure TBDTs with a yield of 0.2–3.6 mg per litre of bacterial culture. Although the yield of FauA was only 0.2 mg per litre of culture, this amount was sufficient to test hundreds of crystallization conditions by mixing small volumes of the protein with identical volumes of crystallization solutions.

3.3. Crystallization and data collection

A survey of crystallization conditions for membrane proteins (http://site.voila.fr/d.cobessi/MPR.html) showed that most of the membrane proteins that fold in β-barrels crystallize using C_8E_4, C_8E_5 or β-octylglucoside as detergents, whereas most of the membrane proteins with a transmembrane domain that folds in α-helices crystallize using sugar-based detergents. Therefore, by predicting the fold of the transmembrane domain, we can probably select the most suitable detergent for crystallization. We used three different

Table 1
Number of crystallization conditions of FauA obtained using three detergents and four sparse matrices.

	Classics Suite	Classics Lite Suite	MbClass Suite	MbClass II Suite
0.75% C_8E_4	1	5	6	8
0.75% C_8E_5	1	5	5	5
1.4% β-OG	0	0	0	0

detergents with different critical micelle concentrations. By combining two to four sparse matrices with three detergents, we tested 576–1152 crystallization conditions using only 30–60 µl purified protein at a concentration of 10 mg ml^{-1}. The best results for FauA were obtained using the MbClass Suite and MbClass II Suite sparse matrices (Table 1) and 0.75% C_8E_4 or C_8E_5. No crystals were obtained with β-octylglucoside, whereas more than ten successful crystallization conditions were obtained using the MbClass Suite or MbClass II Suite sparse matrices with C_8E_4 or C_8E_5. After optimizing the crystallization conditions for FauA, we obtained crystals that were suitable for X-ray studies using 10 mg ml^{-1} FauA in 0.75% C_8E_4 mixed with an equal volume of 0.1 *M* HEPES pH 7.5, 0.3–0.5 *M* ammonium sulfate and 13–17% MPD. The crystals grew slowly, reaching their maximal size in one week. The FauA crystals were frozen in a solution containing a higher MPD concentration or in the same solution with 20% glycerol. Data were first collected on BM30A at the ESRF and subsequently on PROXIMA-I at SOLEIL at 2.3 Å resolution. The high brightness of this beamline allowed us to collect data to a higher resolution than on BM30A using small crystals of membrane protein, typically 0.1 × 0.05 × 0.05 mm in size (Fig. 2 and Table 2). Systematic absences ($2n + 1$) were observed for the 00*l* reflections, resulting from the presence of a 2_1 axis. The crystals belonged to space group $C222_1$, with unit-cell parameters $a = 165.89$, $b = 188.85$, $c = 62.44$ Å.

3.4. The FauA structure and structure quality

FauA is a 77.6 kDa TBDT (699 residues in the mature protein) and 572 residues were rebuilt in the $3F_o - 2F_c$ electron-density map. Several extracellular loops (loops L2, L3, L4, L5, L10 and L11) as well as residues of the TonB box and the N-terminal part were not observed in the electron-density map (see below). Similar to the structure of other TBDTs (Krewulak & Vogel, 2008), FauA can be divided into two domains: a 22-stranded antiparallel transmembrane β-barrel (Phe161–Tyr652) which is filled by an N-terminal plug domain (Glu21–Glu160) (Fig. 3). The r.m.s. deviations calculated using *MSDFold* (Krissinel & Henrick, 2004) range from 1.40 Å (FauA/FptA) to 2.47 Å (FauA/FepA). The main differences are in the length and orientation of the extracellular loops and in the N-terminal part of the plug domain containing the TonB box. 136 water molecules and two sulfate ions from the crystallization conditions were unambiguously identified in the electron-density map. A strong positive peak of electron density was observed close to His288 and Asp290 just up to the girdle of aromatic residues delineating the outer leaflet of the outer membrane. Its position suggests that it could be a phosphate group from a lipid. One molecule is present in the asymmetric unit and symmetry-related FauA molecules interact *via* their hydrophilic parts. The crystals are type II membrane-protein crystals (Michel, 1983) and contain 60.5% solvent. A high solvent content is one of the characteristics of type II membrane-protein crystals. At the end of the refinement, the R and R_{free} values (Brünger, 1992) were 21.9% and 25.8%, respectively. The B-factor average was 45.4 Å^2 for the main chain and 45.9 Å^2 for the overall structure (Table 3).

Table 2
X-ray data statistics.

Values in parentheses are for the highest resolution shell.

	BM30A	PROXIMA-1
Wavelength (Å)	0.9797	0.9789
Resolution (Å)	43.9–3.00 (3.05–3.00)	29.42–2.33 (2.40–2.33)
Space group	$C222_1$	$C222_1$
Unit-cell parameters (Å)	$a = 163.195$, $b = 190.051$, $c = 62.254$	$a = 165.893$, $b = 188.847$, $c = 62.437$
Total reflections	103798 (2995)	308340 (25960)
Unique reflections	19495 (871)	42320 (3521)
Completeness (%)	98.0 (93.5)	99.8 (100)
$\langle I/\sigma(I)\rangle$	11.71 (2.11)	19.88 (2.92)
R_{merge}† (%)	12.0 (62.5)	6.6 (72.4)

† $R_{merge} = \sum_{hkl}\sum_i |I_i(hkl) - \langle I(hkl)\rangle| / \sum_{hkl}\sum_i I_i(hkl)$, where $I_i(hkl)$ is the intensity of the measured reflection and $\langle I(hkl)\rangle$ is the mean intensity of this reflection.

3.5. Flexibility in FauA and other TBDTs

Only five extracellular loops were observed in the $3F_o - 2F_c$ electron-density map. The β-strands of the barrel are connected by long extracellular loops in TBDTs. The length of these loops and their amino-acid content could probably result in flexibility of the loops, as observed in CirA (Buchanan *et al.*, 2007), FepA (Buchanan *et al.*, 1999) and apo BtuB (Chimento *et al.*, 2003). Moreover, the absence of ferric alcaligin or apo alcaligin bound in the binding pocket at the extracellular face of FauA could increase the flexibility of the binding site and extracellular loops, whereas in apo FhuA, FecA or FpvA the loops are observed in the electron density (Locher *et al.*, 1998; Yue *et al.*, 2003; Cobessi, Celia, Folschweiller *et al.*, 2005). In

Figure 2
FauA crystals. Their size is 0.1 × 0.05 × 0.05 mm.

apo FauA, no electron density corresponding to the TonB box is observed. In the crystal structures of apo TBDTs (BtuB, FecA, FpvA, FhuA and CirA) or those bound to their cognate empty siderophore (FecA and FpvA), residues of the TonB box are observed in the electron density. In all the TBDT structures, iron–siderophore binding leads to a conformational change in the N-terminus and flexibility of the TonB box. This flexibility is probably important for interactions with the inner membrane protein TonB. Indeed, the number of TBDTs in the outer membrane is higher than the number of TonB proteins in the inner membrane. The flexibility of the TonB box could thus increase the probability of interactions between the two proteins. The flexibility of the TonB box is an inherent characteristic of TBDTs, including FauA, and does not depend on the ligand-binding status of the transporter. If interactions were to occur between TonB and empty TBDTs, they could lead to energy loss since no membrane transport would occur. Therefore, combined with the increase in flexibility of the TonB box after ligand binding at the extracellular face, other parts of the TBDTs are probably important for the signal tranduction necessary to obtain the energy required for transport. These could include the extracellular loops and the apex of the plug, which undergo conformational changes upon iron–siderophore binding as observed in FpvA, FhuA or FecA. Together, these conformational changes could favour the energy transfer for transport across the outer membrane. Energy transfer may result in partial or total dislocation of the plug to create sufficient space in the lumen of the β-barrel for the passage of large molecules such as the iron–alcaligin complex.

Table 3
Refinement and model statistics.

Values in parentheses are for the highest resolution shell.

Resolution range (Å)	29.35–2.33 (2.39–2.33)
No. of reflections used for R_{cryst} calculation	40176 (2897)
No. of reflections used for R_{free} calculation	2141 (144)
Data cutoff $F/\sigma(F)$	0.0
R_{cryst}† (%)	21.89 (26.90)
R_{free}† (%)	25.84 (36.30)
No. of non-H protein atoms	4384
No. of sulfate ions	2
Mean B factor, protein main-chain atoms (Å^2)	45.28
Mean B factor, protein side-chain atoms (Å^2)	46.42
Ramachandran plot	
Residues in most favoured regions (%)	90.4
Residues in additionally allowed regions (%)	8.2
Residues in generously allowed regions (%)	0.4
Residues in disallowed regions (%)	1.0
R.m.s. deviations from ideal geometry	
Bond lengths (Å)	0.015
Bond angles (°)	1.565

† $R_{cryst} = \sum ||F_{obs}| - |F_{calc}|| / \sum |F_{obs}|$. R_{free} (Brünger, 1992) is the same as R_{cryst} but calculated for n% of data omitted from the refinement; n was 5.1% for FauA.

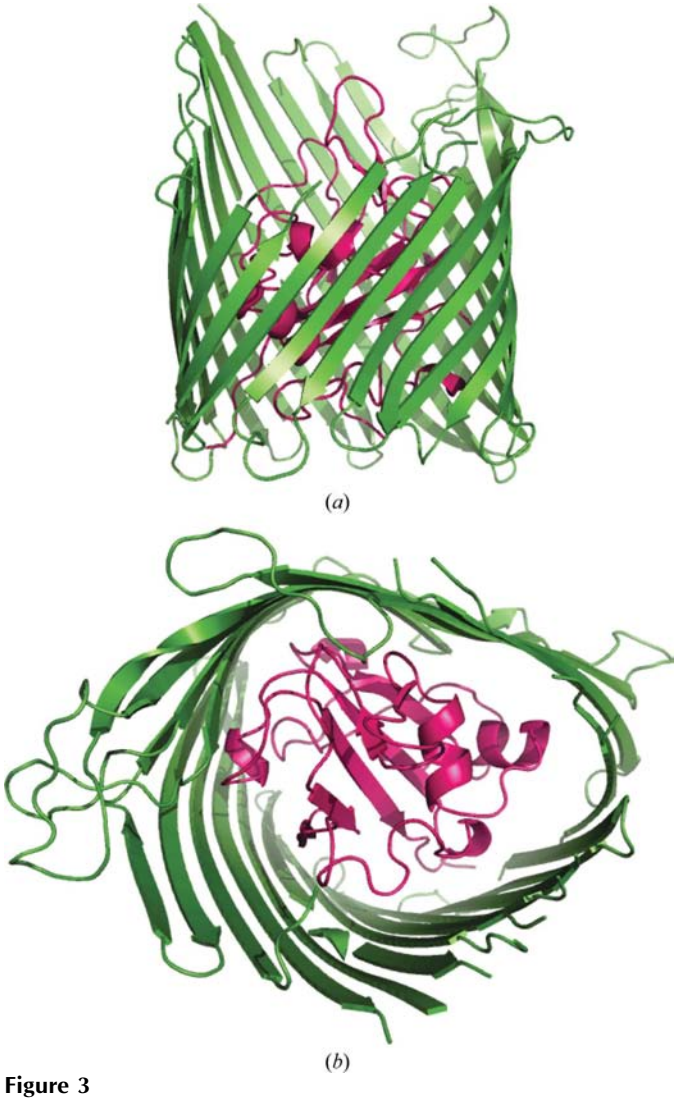

Figure 3
Overall structure of FauA. The plug and the barrel are coloured pink and green, respectively. (*a*) FauA viewed as in the outer membrane, with the extracellular loops at the top and the region exposed to the periplasm at the bottom of the figure. (*b*) View along the β-barrel.

Our customized cloning-to-crystallization protocol for TonB-dependent outer membrane transporters was used to successfully crystallize FauA, the ferric alcaligin receptor of *B. pertussis*, and to solve its three-dimensional structure at high resolution. This approach could be applied to other membrane proteins since the insertion of the His_6 tag in an extracellular hydrophilic loop should not interfere with the secretion process required for protein insertion into the membrane lipid bilayer. A rational design of crystallization experiments using small amounts of membrane proteins purified by a simplified two-step procedure allowed us to find conditions under which crystals suitable for X-ray diffraction could be obtained. Following this expression, purification and crystallization protocol, we also obtained crystals and X-ray diffraction data for three other selected TBDTs (ShuA, SuxA and FetA). Phasing and optimization of the crystallization conditions to reach the highest resolution limits are in progress. Together, these studies will lead to a better understanding of transport and signal transduction across the outer membrane by TBDTs and improve the crystallization methodology of membrane proteins in general.

We thank Sandra Armstrong from the Department of Microbiology, University of Minnesota, Minnesota, USA for

providing *fauA* DNA and for her assistance with the manuscript. We thank the staffs of the PROXIMA-1 beamline at SOLEIL and BM30A at the ESRF for their kind assistance during data collection and the 'European Community-Research Infrastructure Action' under FP6 'Structuring the European Research Area Programme' contract RII3/CT/2004/5060008. This work was supported by the ACI Interface Physique, Chimie, Biologie and the Dynamique et Réactivité des Assemblages Biologiques program of the Ministère de l'Enseignement Supérieur, de la Recherche et de la Technologie and the Centre National de la Recherche Scientifique.

References

Blanvillain, S., Meyer, D., Boulanger, A., Lautier, M., Guynet, C., Denancé, N., Vasse, J., Lauber, E. & Arlat, M. (2007). *PloS ONE*, **2**, 1–21.

Brickman, T. J. & Armstrong, S. K. (1999). *J. Bacteriol.* **181**, 5958–5966.

Brillet, K., Journet, L., Celia, H., Paulus, L., Stahl, A., Pattus, F. & Cobessi, D. (2007). *Structure*, **15**, 1383–1391.

Brünger, A. T. (1992). *Nature (London)*, **355**, 472–475.

Brünger, A. T., Adams, P. D., Clore, G. M., DeLano, W. L., Gros, P., Grosse-Kunstleve, R. W., Jiang, J.-S., Kuszewski, J., Nilges, M., Pannu, N. S., Read, R. J., Rice, L. M., Simonson, T. & Warren, G. L. (1998). *Acta Cryst.* D**54**, 905–921.

Buchanan, S. K., Lukacik, P., Grizot, S., Ghirlando, R., Ali, M. M., Barnard, T. J., Jakes, K. S., Kienker, P. K. & Esser, L. (2007). *EMBO J.* **26**, 2594–2604.

Buchanan, S. K., Smith, B. S., Vankatramani, L., Xia, D., Esser, L., Palniktar, M., Chakraborty, R., van der Helm, D. & Deisenhofer, J. (1999). *Nature Struct. Biol.* **6**, 56–63.

Chimento, D. P., Mohanty, A. K., Kadner, R. J. & Wiener, M. C. (2003). *Nature Struct. Biol.* **10**, 394–401.

Cobessi, D., Célia, H., Folschweiller, N., Heymann, M., Schalk, I., Abdallah, M. & Pattus, F. (2004). *Acta Cryst.* D**60**, 1467–1469.

Cobessi, D., Célia, H., Folschweiller, N., Schalk, I. J., Abdallah, M. A. & Pattus, F. (2005). *J. Mol. Biol.* **347**, 121–134.

Cobessi, D., Célia, H. & Pattus, F. (2004). *Acta Cryst.* D**60**, 1919–1921.

Cobessi, D., Célia, H. & Pattus, F. (2005). *J. Mol. Biol.* **352**, 893–904.

Collaborative Computational Project, Number 4 (1994). *Acta Cryst.* D**50**, 760–763.

Deisenhofer, J., Epp, O., Miki, K., Huber, R. & Michel, H. (1985). *Nature (London)*, **318**, 618–624.

Emsley, P. & Cowtan, K. (2004). *Acta Cryst.* D**60**, 2126–2132.

Ferguson, A. D., Breed, J., Diederichs, K., Welte, W. & Coulton, J. W. (1998). *Protein Sci.* **7**, 1636–1638.

Ferguson, A. D., Chakraborty, R., Smith, B. S., Esser, L., van der Helm, D. & Deisenhofer, J. (2002). *Science*, **295**, 1715–1719.

Ferguson, A. D., Hofmann, E., Coulton, J. W., Diederichs, K. & Welte, W. (1998). *Science*, **282**, 2215–2220.

Hooft, R. W. W., Vriend, G., Sander, C. & Abola, E. E. (1996). *Nature (London)*, **381**, 272.

Kabsch, W. (1993). *J. Appl. Cryst.* **26**, 795–800.

Krewulak, K. D. & Vogel, H. J. (2008). *Biochim. Biophys. Acta*, **1778**, 1781–1804.

Krissinel, E. & Henrick, K. (2004). *Acta Cryst.* D**60**, 2256–2268.

Laskowski, R. A., MacArthur, M. W., Moss, D. S. & Thornton, J. M. (1993). *J. Appl. Cryst.* **26**, 283–291.

Locher, K. P., Rees, B., Koebnik, R., Mitschler, A., Moulinier, L., Rosenbusch, J. P. & Moras, D. (1998). *Cell*, **95**, 771–778.

Loll, P. J. (2003). *J. Struct. Biol.* **142**, 144–153.

Michel, H. (1983). *Trends Biochem. Sci.* **8**, 56–59.

Murshudov, G. N., Vagin, A. A. & Dodson, E. J. (1997). *Acta Cryst.* D**53**, 240–255.

Roth, M., Carpentier, P., Kaïkati, O., Joly, J., Charrault, P., Pirocchi, M., Kahn, R., Fanchon, E., Jacquamet, L., Borel, F., Bertoni, A., Israel-Gouy, P. & Ferrer, J.-L. (2002). *Acta Cryst.* D**58**, 805–814.

Schauer, K., Rodionov, D. A. & de Reuse, H. (2008). *Trends Biochem. Sci.* **22**, 330–338.

Vagin, A. & Teplyakov, A. (1997). *J. Appl. Cryst.* **30**, 1022–1025.

Wiener, M. C. (2005). *Curr. Opin. Struct. Biol.* **15**, 394–400.

Yue, W. W., Grizot, S. & Buchanan, S. K. (2003). *J. Mol. Biol.* **332**, 353–368.